

Vibrational Spectroscopy of the Three Isomers of 1,4-Difluorobutadiene

Norman C. Craig,* Christopher F. Neese, Tuan N. Nguyen, Catherine M. Oertel, and Laura Pedraza

Department of Chemistry, Oberlin College, Oberlin, Ohio 44074

Anne M. Chaka

The Lubrizol Corporation, Wickliffe, Ohio 44092-2298

Received: April 26, 1999; In Final Form: June 28, 1999

Infrared and Raman spectra were recorded for the *trans,trans* (*EE*), *cis,cis* (*ZZ*), and *cis,trans* (*ZE*) isomers of 1,4-difluorobutadiene (DFBD). From these spectra and frequencies predicted from the adiabatic connection method, which is a hybrid of Hartree–Fock and density–functional theories, complete assignments of fundamentals were made for the observable *s-trans* configurations. The fundamentals for the *trans,trans* isomer are (in cm^{-1}): (a_g) 3091, 3048, 1681, 1325, 1280, 1151, 1121, 409, 383; (a_u) 934, 798, 227, 154; (b_g) 897, 830, 397; and (b_u) 3086, 3056, 1638, 1299, 1221, 1088, 621, 133. The fundamentals for the *cis,cis* isomer are (in cm^{-1}): (a_g) 3118, 3088, 1676, 1410, 1248, 1134, 946, 751, 232; (a_u) 914, 762, 330, 78; (b_g) 897, 789, 580; and (b_u) 3109, 3092, 1624, 1340, 1215, 1044, 632, 165. The fundamentals for the *cis,trans* isomer are (in cm^{-1}): (a') 3114, 3082, 3062, 3036, 1690, 1629, 1391, 1313, 1253, 1224, 1138, 1129, 1008, 706, 504, 308, 138; and (a'') 929, 887, 824, 758, 526 (calculated), 230, 155. Overall agreement between the assignments and the predicted frequencies is quite good. With allowance for the difference between modes strongly dependent on CF or CCl motions, a very good correlation was found between the fundamentals of the three isomers of DFBD and the corresponding isomers of 1,4-dichlorobutadiene. Both sets of isomers are of special interest because they exhibit the *cis* effect, in which the *cis,cis* isomer has the lowest energy and the *trans,-trans* isomer has the highest energy.

Introduction

From the initial work of Viehe and Franchimont in 1963, the isomers of 1,4-difluorobutadiene (DFBD) are known to have an unusual equilibrium relationship in which the *cis,cis* isomer is favored ("mit bevorzugter *cis*-Struktur"), the so-called *cis* effect.^{1,2} Thus, at temperatures in the range 100–150 °C, the *cis,cis* (*ZZ*) isomer is the most stable, and the *trans,trans* (*EE*) isomer is the least stable, despite the greater electronic crowding in the *cis,cis* isomer. The *cis,trans* (*ZE*) isomer has intermediate stability. With the van't Hoff equation, we have analyzed the reported equilibrium compositions and have found the experimental energy differences at 125 °C given in Figure 1.^{2,3} These energy differences show that the *cis,cis* isomer has the lowest energy, and the *trans,trans* isomer the highest energy in accord with the trend in equilibrium compositions with increasing temperature. With a hybrid Hartree–Fock/density–functional theory, specifically the adiabatic connection method (ACM) proposed by Becke,⁴ we computed the energies for these three isomers and found the calculated values given in Figure 1. These calculated energy differences, which include differences in thermal energies at 298 K and differences in zero-point vibrational energies, not only encompass the seemingly anomalous energy relationships among the isomers but are in rather good agreement with the values derived from experiment. Thus, the curious *cis* effect is contained within practical quantum mechanics, even though no accepted qualitative theory anticipates the result.

An even more arresting example of the *cis* effect is found among the isomers of 1,4-dichlorobutadiene. Viehe and Franchimont also investigated the temperature-dependent equi-

bria in this system.^{1,2} The *cis,cis* isomer is 11.4 kJ/mol lower in energy than the *trans,trans* isomer, as computed by us from the published equilibrium data. The vibrational spectra of the isomers of 1,4-dichlorobutadiene have been thoroughly studied by Benedetti et al.,⁵ who assigned vibrational fundamentals for all three isomers.

The overall goal of the research, of which this report is a part, is to obtain relevant experimental data that might suggest new qualitative theories or be a basis for testing proposed theories to explain the curious *cis* preference in the 1,4-difluorobutadienes and a similar, *gauche* effect in related molecules.^{6,7} The present paper reports infrared (IR) and Raman spectra and assignments of vibrational fundamentals for the three isomers of DFBD. From the results of the ACM, force-constant calculations and normal-mode analyses on fully optimized geometries, frequencies of vibrational fundamentals and intensities for IR transitions were predicted. These predictions have helped substantially in arriving at nearly complete assignments of fundamentals for all three isomers of DFBD from experimental data.

We are also engaged in studies to determine the detailed structures of the three isomers. For the nonpolar *trans,trans* and *cis,cis* isomers, high-resolution IR spectroscopy is being applied, a method that has successfully been used in the study of several small molecules that exhibit the *cis* or *gauche* effect between isomers or rotamers.⁸ For the polar *cis,trans* isomer, microwave spectroscopy is being applied.

Our preparation of *trans,trans*-DFBD was by a different method than that used by Viehe and Franchimont.² They reacted fluoroethylene with 1-fluoro-2-iodoethylene photochemically

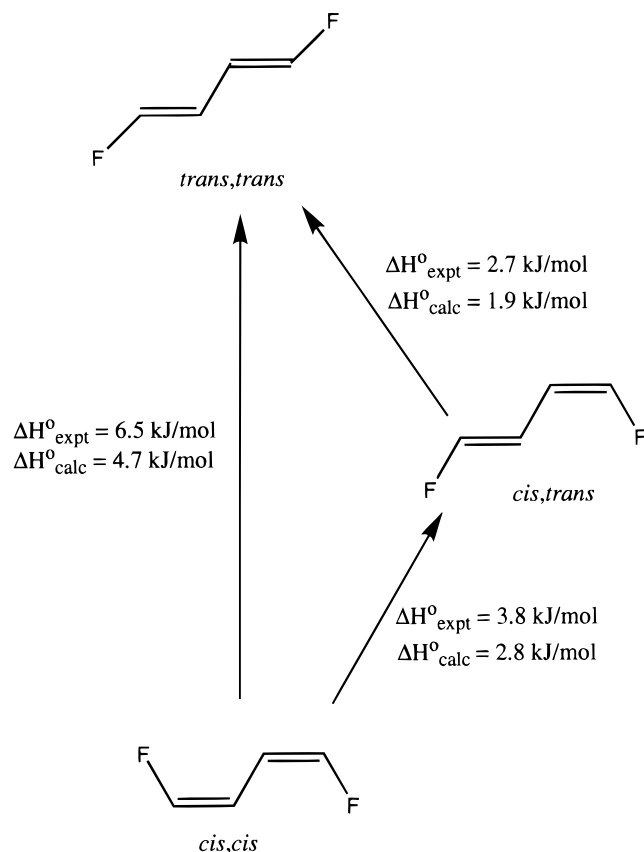


Figure 1. Energy relationships among the three isomers of 1,4-difluorobutadiene. Calculated values are from the ACM and include thermal energies at 298 K and zero-point vibrational energies.

and then used reaction with base to remove hydrogen iodide and form a mixture of the isomers of DFBD. Our method of synthesis of *trans,trans*-DFBD was by the stereospecific isomerization of *trans*-3,4-difluorocyclobutene, the synthesis of which we have previously reported.⁹ This isomerization reaction is similar to the known electrocyclic ring opening of *trans*-3,4-dichlorocyclobutene to *trans,trans*-1,4-dichlorobutadiene.¹⁰ Following the method of Viehe and Franchimont, we used iodine catalysis to convert *trans,trans*-DFBD into an equilibrium mixture of the three isomers, which are separable by gas chromatography.

Experimental Section

Synthesis and Characterization. The *trans* isomer of 3,4-difluorocyclobutene was prepared from *cis*-3,4-dichlorocyclobutene by bulb-to-bulb distillation through a column containing a mixture of silver difluoride and potassium fluoride solids.⁹ About 1 mmol of purified *trans*-DFCB was isomerized to *trans,trans*-DFBD in a stopcock-equipped bulb in the gas phase by heating at 70 °C for 12 h. The stopcock, lubricated with Silicone grease, was kept at room temperature. Because *trans*-DFCB and *trans,trans*-DFBD are difficult to separate by gas chromatography (GC), it is best to let the isomerization go nearly to completion.

trans,trans-DFBD was converted into a mixture of the three isomers by heating 1–2 mmol with a few crystals of iodine in a stopcock-equipped bulb at 100 °C for 24 h. The stopcock, greased with Krytox, was kept at room temperature. Alternatively, heating *trans*-DFCB under the same conditions leads directly to the mixture of isomers. Iodine was removed from the reaction products by distilling them through a tube containing

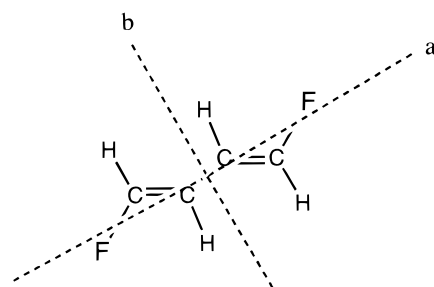


Figure 2. Schematic location of the principal axes for *trans,trans*-1,4-difluorobutadiene. The *c* axis passes through the center of symmetry and is perpendicular to the molecular plane.

TABLE 1: Predicted Principal Moments of Inertia of the Isomers of 1,4-Difluorobutadiene (in amu Å²)

isomer	I_a	I_b	I_c	κ^a
<i>trans,trans</i> -DFBD	15.708	431.208	446.917	-0.9973
<i>cis,cis</i> -DFBD	36.703	317.920	354.624	-0.9734
<i>cis,trans</i> -DFBD	37.996	346.449	384.446	-0.9759

^a Asymmetry parameter, $\kappa = (2B - A - C)/(A - C)$, where $A = h/(8\pi^2cI_a)$, etc.

fine copper metal turnings. The three isomers were separated by GC at room temperature on a 5-m column packed with Fluoropak coated with 10% tricresyl phosphate. The relative elution times were 1.0 for *cis,cis*-DFBD, 1.4 for *cis,trans*-DFBD, and 1.7 for *trans,trans*-DFBD. More than one pass was needed to completely separate the *trans,trans* and *cis,trans* isomers. Finally, samples were dried by distillation through a column containing phosphorus pentoxide. The samples of the *trans,trans* isomer used in spectroscopy contained a small amount of residual *trans*-DFCB, for which IR bands are known.⁹

For the most part, we had success in storing the purified DFBD samples in a deep freeze at -15 °C. After experiencing polymerization of the *cis,cis* isomer on one occasion, we used a few crystals of hydroquinone as an inhibitor. Such treatment made possible mailing samples to Germany for high-resolution spectroscopy.

Boiling points were estimated by measuring vapor pressures at temperatures below room temperature and using the Clausius–Clapeyron equation to make an extrapolation. The boiling points are 32 °C for the *cis,cis* isomer, 38 °C for the *cis,trans* isomer, and 41 °C for the *trans,trans* isomer and are in the same order as the GC elution times. Melting points were estimated in the Raman studies by using the cessation of scattering of the laser beam to tell when the last material had melted. The melting points are -56 °C for the *trans,trans* isomer, -58 °C for the *cis,cis* isomer, and -96 °C for the *cis,trans* isomer, which is the lower-symmetry molecule with the substantially lower melting point, as expected.

For the *trans,trans* isomer, the proton nuclear magnetic resonance (NMR) spectrum was a complex multiplet at 5.83 ppm and a complex doublet (d) of multiplets at 6.75 ppm, with an overall splitting of ~81 Hz. The ¹⁹F spectrum was a complex d of multiplets at -126.28 ppm, with an overall splitting of ~81 Hz. The ¹³C spectrum consisted of a dd (265.7, 17.4 Hz) at 151.00 ppm and a dd (15.4, 15.2 Hz) at 106.14 ppm. For the *cis,cis* isomer, the proton spectrum was a complex d of multiplets at 5.74 ppm, with an overall splitting of ~40 Hz, and a complex d of multiplets at 6.44 ppm, with an overall splitting of ~81 Hz. The ¹⁹F spectrum was a complex quartet (q) of multiplets at -125.03 ppm, with splittings of ~81 and ~40 Hz. The ¹³C spectrum consisted of a dd (268.7, 5.6 Hz) at 148.07 ppm and a dd (5.7, 3.9 Hz) at 101.74 ppm. All the NMR

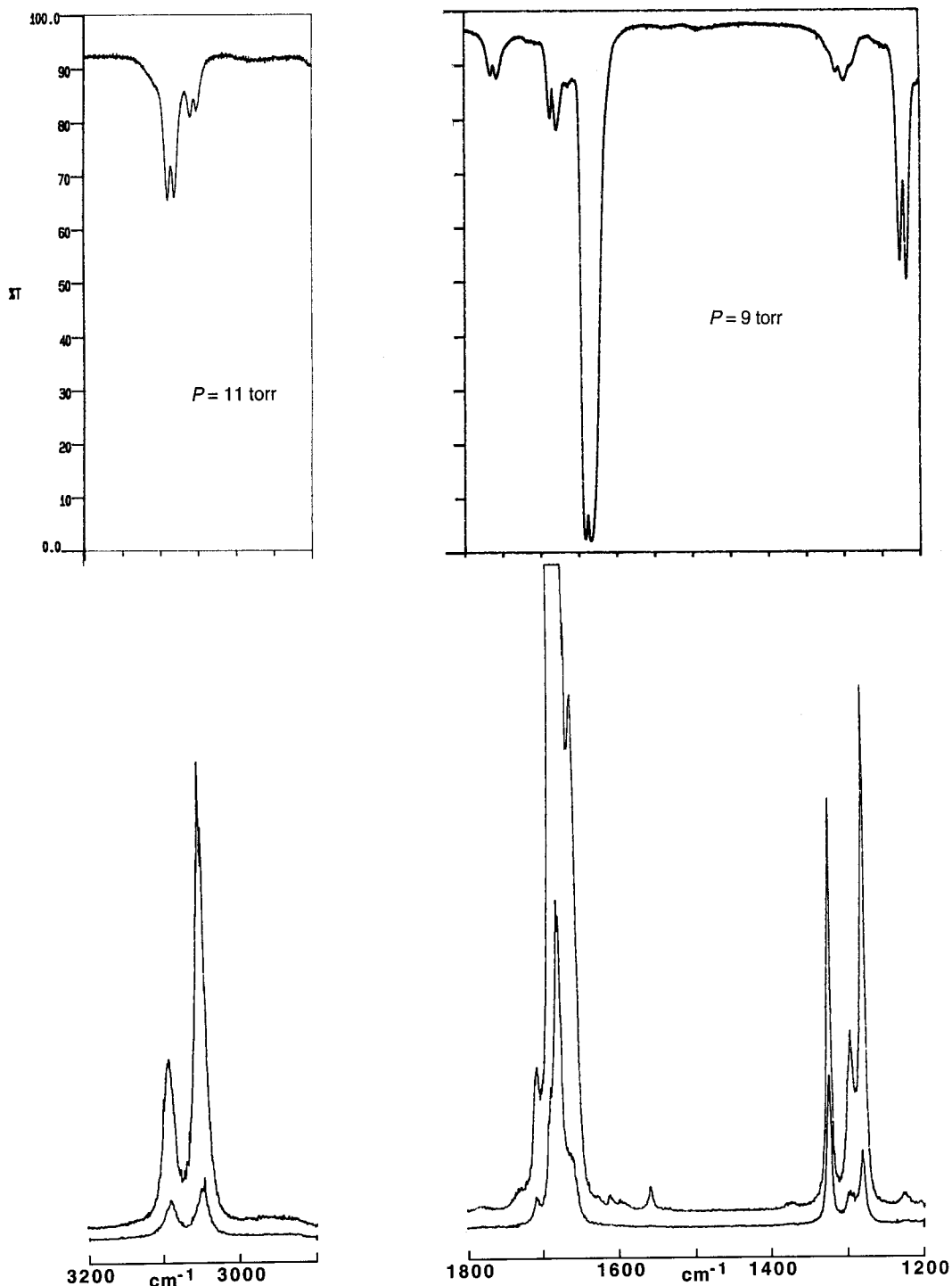


Figure 3. The CH and C=C stretching regions for *trans,trans*-1,4-difluorobutadiene. Gas-phase IR spectrum on top; liquid-phase ($T = -54\text{ }^{\circ}\text{C}$) Raman spectrum on the bottom.

spectra for the *cis,trans* isomer were first order. The proton spectrum was a dddd (39.5, 11.4, 4.8, 1.9, 0.5 Hz) at 5.24 ppm, a dtd (17.3, 11.4, 0.9 Hz) at 6.25 ppm, a ddq (82.5, 4.7, 1.0) at 6.45 ppm, and a dtdt (82.6, 11.2, 1.1, 0.5 Hz) at 6.80 ppm ($t = \text{triplet}$, $q = \text{quartet}$). The ^{19}F spectrum was a dddd (82.5, 17.3, 15.8, 1.7, 1.2 Hz) at -125.04 ppm and a dddd (82.6, 39.6, 15.9, 1.1 Hz) at -126.43 ppm. The ^{13}C spectrum was a dd (262.2, 3.5 Hz) at 151.32 ppm, a dd (265.8, 12.3 ppm) at 148.31 ppm, a dd (18.2, 6.2 Hz) at 104.63 ppm, and a dd (12.2, 3.7 Hz) at 103.60 ppm.

Spectroscopy. Infrared spectra were recorded on Perkin-Elmer FT 1760 and FT 1700X spectrometers, the latter a far-

IR instrument. Wilmad mini gas cells of 10-cm length, with 25-mm diameter cesium iodide or polyethylene windows, were used for gas samples. Resolution was 0.5 cm^{-1} in the mid-IR region and 1 cm^{-1} in the far-IR region. The typical number of scans accumulated was 25 in the mid-IR region and 200 in the far-IR region. Reported frequencies were accurate to at least $\pm 0.5\text{ cm}^{-1}$. Both spectrometers were purged with dry nitrogen.

Raman spectra were excited by the 514.5-nm line from a Coherent Innova 70 argon-ion laser and recorded with a Spex Ramalog 5 system and associated Nicolet 1180 computer. The green laser line was isolated with a home-built Amici prism system or with a Kaiser Optical corner cube. Samples were

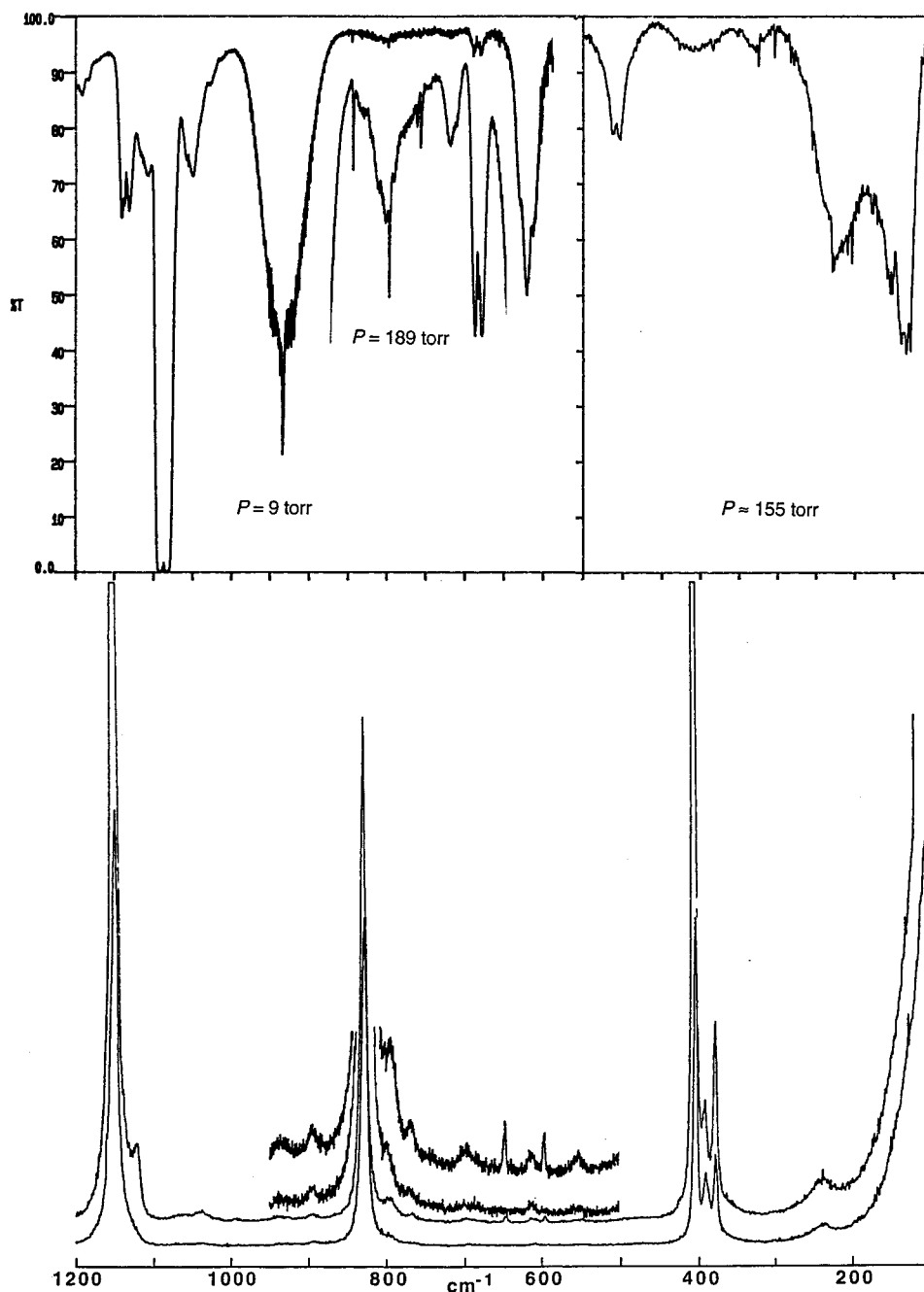


Figure 4. Skeletal motion and low-frequency region for *trans,trans*-1,4-difluorobutadiene.

sealed in 1.8-mm Pyrex capillaries and mounted in a Harney–Miller-type cell to permit continuous cooling with a stream of cold nitrogen gas. Spectra were recorded with a resolution of $\sim 2.5 \text{ cm}^{-1}$, and frequencies are good to $\pm 2 \text{ cm}^{-1}$. For each setting of the polarizer in the 90° -scattered light, 4 scans were accumulated. Spectra shown in this report were treated with a 9-point smoothing function.

Our simple technique for transferring cold capillaries *frost-free* into an already cold Harney–Miller cell has not been described before. In the present work with fluorobutadienes, warming the capillary to room temperature runs the risk of initiating the formation of some fluorescent impurities in the liquid sample. In other cases, samples may have boiling points below room temperature. A cold diethyl ether bath, typically around -50°C , is prepared in a Dewar flask by slowly adding liquid nitrogen to the ether. The capillary sample tube is transferred from cold storage directly into the cold ether. With

a laboratory tissue, frost is wiped off the capillary as the capillary is raised just above the surface of the ether, and the capillary is immersed again in the ether. Then, the capillary tube with its cold ether layer as a protection from frost formation is quickly transferred into the precooled Harney–Miller cell where the ether finishes evaporating.

NMR spectra were recorded on a Bruker AC-200 instrument at room temperature in standard 5-mm tubes with deuteriochloroform as the solvent. External TMS and CF_3Cl were the references.

ab initio Calculations. The ACM used in this work is based on the hybrid exchange–correlation functional proposed by Becke, in which a term representing the exact Hartree–Fock exchange energy is included along with a linear combination of several widely used functionals.⁴ We have used the original coefficients proposed by Becke in the ACM formalism implemented within the TURBOMOLE Program.¹¹ All geometry

TABLE 2: Observed Vibrational Frequencies and Assignments for *trans,trans*-1,4-Difluorobutadiene (in cm^{-1})

infrared			Raman			predicted ^a		assignment	
gas			liquid			freq.	I ^c		
freq.	sh. ^b	I ^c	freq.	pol. ^d	I ^c			freq.	I ^c
3086	B(9.0)	m	3091	p	w	3210		ν_1 fundamental	a _g
3056	B(8.6)	wm				3210	m	ν_{17} fundamental	b _u
						3189	wm	ν_{18} fundamental	b _u
			3048	p	m	3182		ν_2 fundamental	a _g
			1681	p	vs	1745		ν_3 fundamental	a _g
1638	B(7.3)	vs				1692	s	ν_{19} fundamental	b _u
			1325	p	m	1351		ν_4 fundamental	a _g
1306	B(10.5)	wm				1334	w	av 1299 ν_{20} fund.	b _u
1291	B(11)	wm						$\nu_6 + \nu_{24} = 1284$ FR ^e	B _u
			1297	p	w			$\nu_{14} + \nu_{16} = 1294$ FR ^d	A _g
			1280	p	m	1315		ν_5 fundamental	a _g
1221	B(8.7)	ms				1243	m	ν_{21} fundamental	b _u
			1151	p	s	1183		ν_6 fundamental	a _g
1137	A/B(9.3)	m						$\nu_{12} + \nu_{14} = 1124$ FR ^e	B _u
			1121	p	w	1176		ν_7 fundamental	a _g
1088	A/B(7.7)	vs				1107	vs	ν_{22} fundamental	b _u
934	C(24)	s				970	s	ν_{10} fundamental	a _u
			897	dp?	vvw	910		ν_{14} fundamental	b _g
			830	dp?	m	865		ν_{15} fundamental	b _g
798	C(16)	w				831	vw	ν_{11} fundamental	a _u
621	?(16.2)	ms				624	m	ν_{23} fundamental	b _u
								$\nu_{12} + \nu_{16} = 624$ FR ^e	B _u
506	A/B(7.8)	vw						$\nu_9 + \nu_{24} = 516$	B _u
			409	p	s	410		ν_8 fundamental	a _g
			397	dp	w	402		ν_{16} fundamental	b _g
			383	p	m	385		ν_9 fundamental	a _g
			245	p	vw			$2 \times \nu_{24} = 266$	A _g
227	C(24) ^f	w				238	w	ν_{12} fundamental	a _u
154	C?	w				127	vvw	ν_{13} fundamental	a _u
133	A/B?(12)	w				146	w	ν_{24} fundamental	b _u

^a Predicted frequency and IR intensity from ACM calculations. Computed relative IR intensities were, in order of decreasing frequency within a symmetry species: (a_u) 31.12, 0.30, 0.94, 0.04; and (b_u) 5.33, 3.32, 48.53, 1.76, 11.46, 100.00, 11.06, 1.05. ^b Band shape; P–R spacing in parentheses; Q = based on Q branch only; br = broad. ^c Intensity: vs = very strong; s = strong; m = medium; wm = weak medium; w = weak; vw = very weak; vvw = very very weak; sh = shoulder. ^d Depolarization ratio: p = polarized; dp = depolarized. ^e FR = Fermi resonance. ^f Probable structure on low frequency side of band.

optimizations and vibrational frequency calculations were performed using basis sets of triple- ζ quality plus two sets of polarization functions (tz2p) per atom.¹² No scaling was used in computing the vibration frequencies.

Results

Viehe and Franchimont used low-resolution, gas-phase IR spectra to assign structures to the three isomers of DFBD.² They assumed that the favored rotamer was the s-trans one for each isomer. Two of the IR spectra were sparser, as expected, for the centrosymmetric *trans,trans* and *cis,cis* isomers in comparison with the spectrum of the less symmetric *cis,trans* isomer. In addition, the *trans,trans* isomer has only *trans*-related hydrogen atoms with respect to the double bonds and thus a strong IR band due to out-of-plane CH flapping in the 925- cm^{-1} region. The *cis,cis* isomer has only *cis*-related hydrogen atoms and thus a strong band due to CH out-of-plane flapping in the 760- cm^{-1} region. The *cis,trans* isomer has both *cis*- and *trans*-related hydrogen atoms and thus strong bands due to out-of-plane CH flapping in both spectral locations. In support of this interpretation, similar patterns were found in the spectra of the three isomers of 1,4-dichlorobutadiene.² As shown in the spectra given in the present paper and discussed later, these initial assignments of structures for the three isomers of DFBD have been confirmed by our higher-resolution spectroscopy and by ab initio calculations.

The assignments of structures for the three isomers are also confirmed by the NMR spectra. The spectra for the *trans,trans*

and *cis,cis* isomers have only two types of protons and ¹³C and one type of ¹⁹F. Further, the *cis,cis* isomer shows an HF coupling constant of significant size, as is characteristic of *trans* HC=CF geometry, in addition to the large gem HF coupling constant. For the *cis,trans* isomer, which is of lower symmetry, all of the protons, carbon nuclei, and fluorine nuclei are different.

The ab initio calculations with the ACM showed that the s-*trans* rotamers depicted in Figure 1 are the lower energy forms of each of the three isomers of DFBD. The higher energy forms of the *trans,trans* and *cis,cis* isomers are s-*gauche*, with calculated dihedral angles of 43.6° and 38.2°, respectively. These outcomes are similar to that for butadiene itself for which a dihedral angle of 34.0° is predicted by the ACM for the high-energy rotamer with the skewed structure. Similar results for butadiene have been reported before. Experimental results are consistent with the higher energy form of butadiene being s-*gauche*.^{13,14} With a split valence set and second-order Møller–Plesset (MP2/6-31G*) perturbation theory, De Maré and co-workers predicted an energy difference of 11.2 kJ/mol between the s-*gauche* and s-*trans* rotamers.¹⁴ In addition, they predicted a dihedral angle of 37.8° for the s-*gauche* rotamer. In contrast to the predictions for *trans,trans* and *cis,cis* isomers of DFBD and unsubstituted butadiene, the ACM calculations predict a planar, s-*cis* structure for the higher energy rotamer of *cis,trans*-DFBD. Calculated rotamer energy differences from the ACM are 12.5 kJ/mol for *trans,trans*-DFBD, 19.4 kJ/mol for *cis,cis*-DFBD, and 10.0 kJ/mol for *cis,trans*-DFBD. In each case, these energy differences are sufficiently high that only the s-*trans*

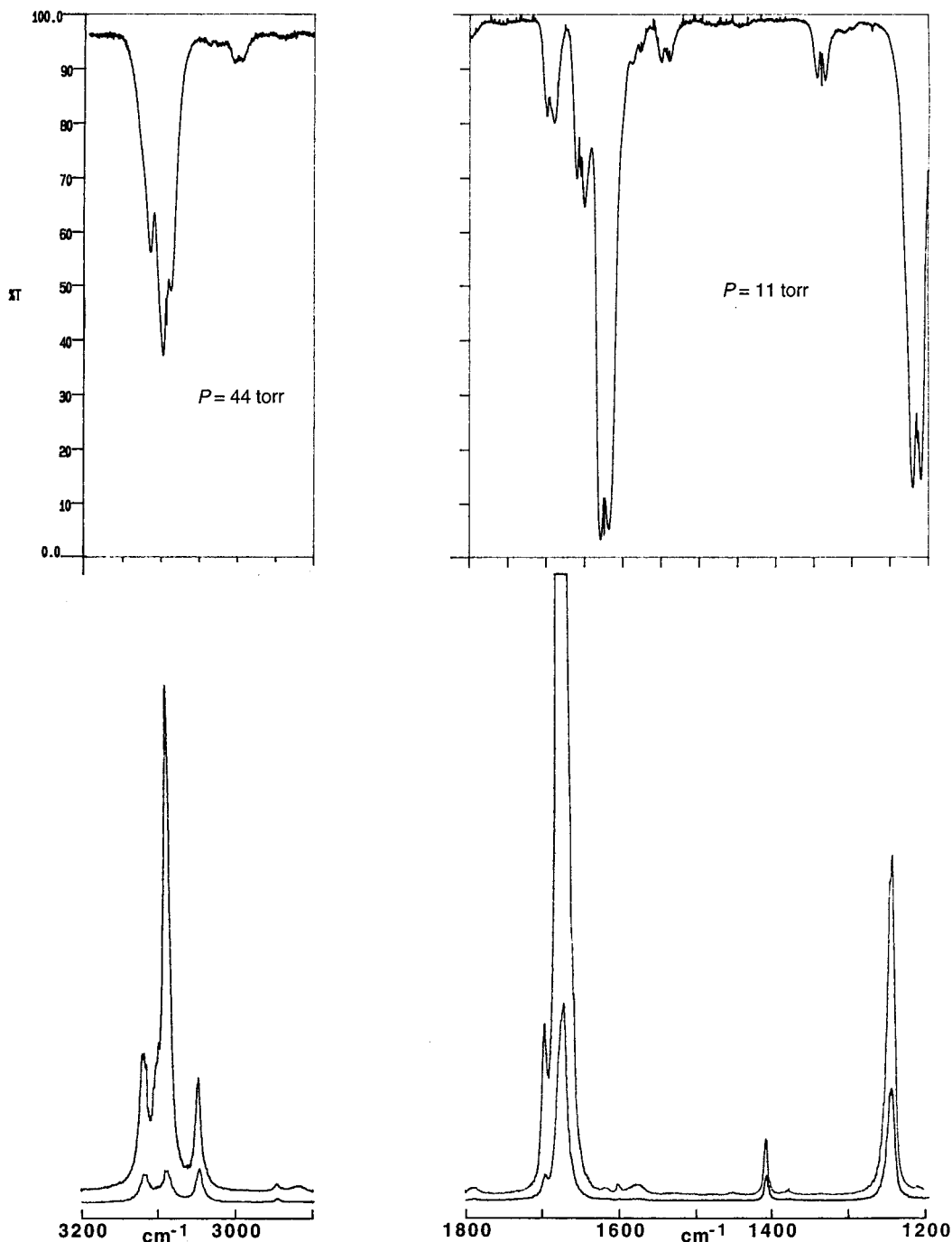


Figure 5. The CH and C=C stretching regions for *cis,cis*-1,4-difluorobutadiene. Gas-phase IR spectrum on top; liquid-phase ($T = -53\text{ }^{\circ}\text{C}$) Raman spectrum on the bottom.

rotamers are expected to be present in normally observable amounts at room temperature and below. (A weak band due to *s-gauche*-butadiene was observed with a 27-m path length at room temperature.¹⁴)

Two of the isomers of DFBD, the *trans,trans* and *cis,cis* isomers, have the same symmetry, C_{2h} , and thus, the same selection rules for vibrational transitions. Table 1 gives the moments of inertia and the corresponding asymmetry parameters, κ , of all three isomers as predicted from the ACM calculations. Calculated Cartesian coordinates and geometric parameters are given in the Supporting Information, Tables S1-S6. The *trans,trans* isomer, with a κ of -0.997 , is very close to a prolate symmetric top. In this centrosymmetric molecule, the *a* axis passes through the center of the molecule and close to both fluorine atoms. The *b* axis also lies in the plane of the

molecule. Figure 2 shows schematically the relationship of the inertial axes to the molecular structure of the *trans,trans* isomer. The centrosymmetric *cis,cis* isomer is a little further from a prolate symmetric top with a κ of -0.973 . For the *cis,cis* isomer, the *a* axis passes through the center of mass and almost parallel to the C=C bonds but slightly tipped toward the fluorine atoms. The *b* axis for this isomer also lies in the plane of the molecule. For both isomers, the fundamental modes consist of nine in-plane vibrations of the a_g symmetry species, four out-of-plane vibrations of the a_u symmetry species, three out-of-plane vibrations of the b_g symmetry species, and eight in-plane vibrations of the b_u symmetry species. Only the a_u and b_u modes are IR active. As a consequence of the orientation of the axes for the principal moments for both isomers, bands due to in-plane modes of b_u symmetry will have hybrid A/B-type shapes

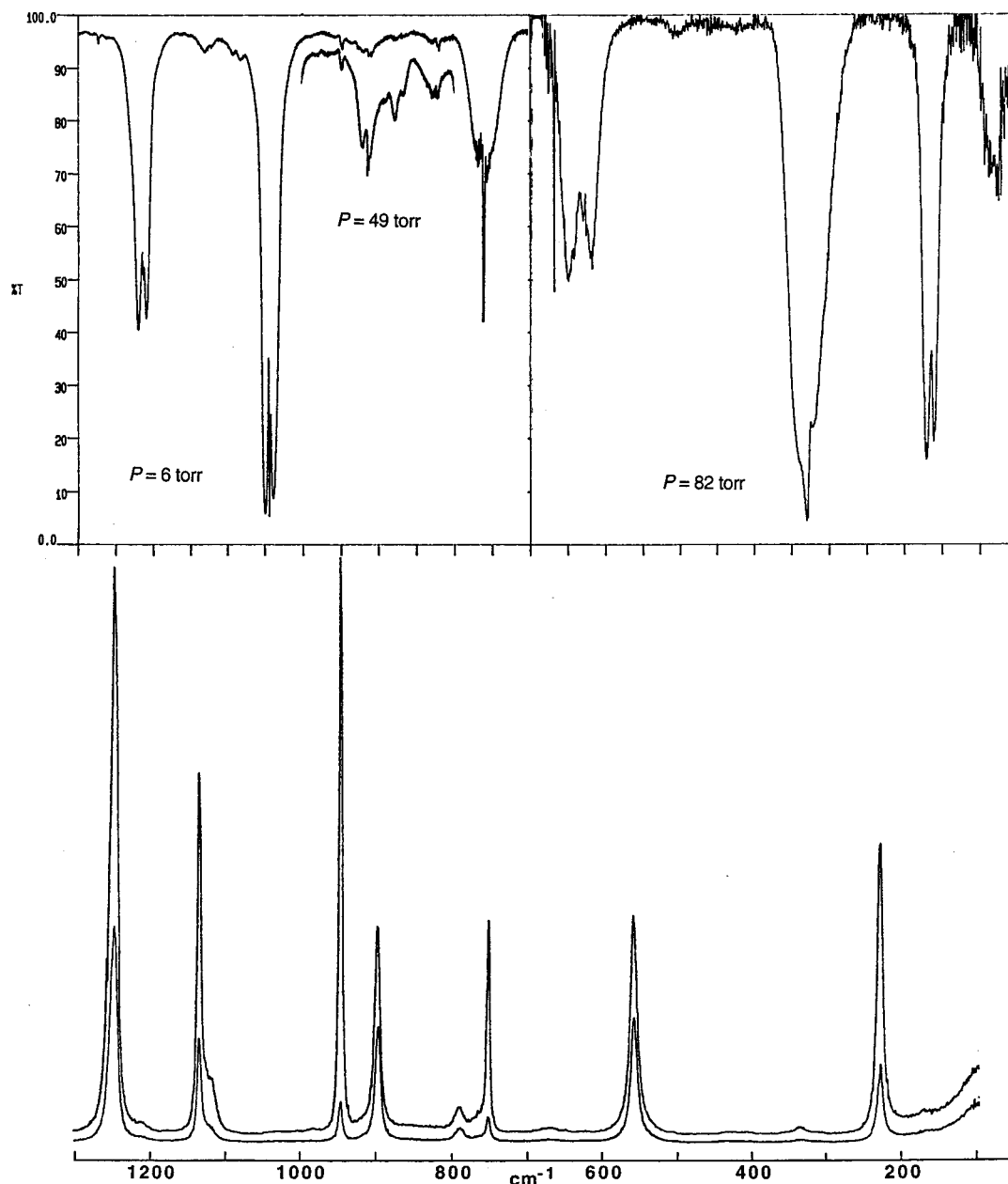


Figure 6. Skeletal motion and low-frequency region for *cis,cis*-1,4-difluorobutadiene.

in gas-phase IR spectra and bands due to out-of-plane modes of a_u symmetry will have C-type shapes. Only the a_g and b_g fundamentals are Raman active. Those bands due to a_g transitions will be polarized, whereas bands due to modes of b_g symmetry species will be depolarized.

The selection rules are different for the *cis,trans* isomer, which has only C_s symmetry. Although this isomer has lower symmetry than the other two isomers, it is also close to a prolate symmetric top with $\kappa = -0.976$. The 17 in-plane fundamental modes belong to the a' symmetry species; the remaining seven out-of-plane modes belong to the a'' symmetry species. All modes are IR and Raman active. Gas-phase IR spectra have hybrid A/B-type band shapes for the a' modes and C-type band shapes for the a'' modes. The a' modes will give polarized Raman bands and the a'' modes depolarized Raman bands.

Assignment for *trans,trans*-DFBD. Infrared and Raman spectra for *trans,trans*-DFBD are shown together in Figures 3 and 4. In each case, the upper trace is the IR spectrum of the gas phase and the lower trace is the Raman spectrum of the

liquid phase. The two traces in the Raman spectrum show the outcome with two settings of the polarization analyzer in the 90° -scattered light. Figure 4 shows additional spectral evidence in support of weak bands for fundamentals in the 900-cm^{-1} region of both the IR and Raman spectra. The added IR segment was recorded at a higher pressure of 189 Torr; the added Raman segment was recorded with eight scans and displayed with more gain and without smoothing. Table 2 gives the assignment of the main bands observed in the IR and Raman spectra. In both spectra, some weak bands are due to residual *trans*-DFCB. Some other, unidentified impurity bands make weak contributions to both spectra. Many of the sharp lines in the far-IR part of the spectrum are due to residual water. In Figure 4, different intensity patterns in the scans at the two pressures in the IR spectrum confirm impurity features in this region. Table 2 includes all the frequencies and the IR intensities as predicted from the ACM calculations. Omitted from Table 2 are assignments for impurities and for combination tones not crucial to

TABLE 3: Observed Vibrational Frequencies and Assignments for *cis,cis*-1,4-Difluorobutadiene (in cm^{-1})

infrared			Raman			predicted ^a		assignment	
gas		<i>I</i> ^c	liquid		<i>I</i> ^c	freq.	<i>I</i> ^c		
freq.	sh. ^b		freq.	pol. ^d					
3109	B(~9)	m	3118	p	w	3232		ν_1 fundamental	a_g
3092	A(10.6)	m				3233	m	ν_{17} fundamental	b_u
						3213	m	ν_{18} fundamental	b_u
			3088	p	s	3205		ν_2 fundamental	a_g
			3047	p	w			$\nu_3 + \nu_4 = 3086$ FR ^e	A_g
			1676	p	vs	1740		ν_3 fundamental	a_g
1624	A(10.5)	vs				1681	vs	ν_{19} fundamental	b_u
			1602	p	vw			¹³ C isotopomer?	
			1410	p	w	1445		ν_4 fundamental	a_g
1340	A(10.5)	m				1364	m	ν_{20} fundamental	b_u
			1248	p	s	1284		ν_5 fundamental	a_g
1215	B(10.3)	s				1244	s	ν_{21} fundamental	b_u
			1134	p	m	1166		ν_6 fundamental	a_g
1044	A(10.8)	vs				1061	vs	ν_{22} fundamental	b_u
			946	p	s	972		ν_7 fundamental	a_g
914	C(15)	w				953	vw	ν_{10} fundamental	a_u
			897	dp	m	934		ν_{14} fundamental	b_g
			789	dp	w	808		ν_{15} fundamental	b_g
762	C16)	s				788	s	ν_{11} fundamental	a_u
			751	p	m	767		ν_8 fundamental	a_g
644	?(~8)	w				643	m	av 632 ν_{23} fund.	b_u
620	?(~7)	w						$\nu_{13} + \nu_{16} = 638$ FR ^e	B_u
			580	dp	m	585		ν_{16} fundamental	b_g
330	C(17)					338	m	ν_{12} fundamental	a_u
			232	p	m	230		ν_9 fundamendal	a_g
165	B(10.4)	m				162	m	ν_{24} fundamental	b_u
78	C?	w				89	w	ν_{13} fundamental	a_u

^a See Table 2 except: (a_u) 0.41, 24.3, 9.35, 0.82; (b_u) 3.06, 2.95, 63.50, 2.58, 39.71, 100.00, 2.16, 2.33. ^{b-e} See Table 2.

the assignment of fundamentals. These additional assignments are in Table S7 in the Supporting Information.

Based on the selection rules, most of the assignments of vibrational fundamentals for the *trans,trans* isomer are straightforward. We comment here only on the assignments that required closer analysis. Three of these exceptions are in the a_g symmetry species. In the absence of the predictions of fundamental frequencies, we would have assigned the lowest frequency a_g mode to the polarized Raman band at 245 cm^{-1} . This frequency is so far below the predicted frequency of 385 cm^{-1} that we selected the polarized Raman band at 383 cm^{-1} for this fundamental. Initially, the band at 383 cm^{-1} had seemed due to a Fermi resonance doublet with the stronger, polarized band at 409 cm^{-1} . The predictions support, however, assigning two a_g modes within 26 cm^{-1} . The 245-cm^{-1} band is now explained as $2 \times \nu_{24} = 266 \text{ cm}^{-1}$, with some allowance for differences in frequencies between the liquid phase and gas phase. Furthermore, the assignment of ν_9 as 383 cm^{-1} gives a good explanation for the weak IR band at 506 cm^{-1} as the combination tone $\nu_9 + \nu_{24} = 516 \text{ cm}^{-1}$.

The calculated fundamentals led to improved assignments of a_g modes in the $1100\text{--}1300\text{-cm}^{-1}$ region. The predicted frequencies for ν_6 and ν_7 were 1183 and 1176 cm^{-1} , respectively. In view of the close proximity of these two predicted frequencies and their location, it seemed best to choose the strong band at 1151 cm^{-1} and the weaker band at 1121 cm^{-1} in the Raman spectrum for these two modes. Use of the alternative of two bands at 1297 cm^{-1} and 1280 cm^{-1} in the Raman spectrum for two a_g fundamentals would not agree nearly as well with the predictions. Furthermore, there is a good explanation for the 1297-cm^{-1} band as the combination tone $\nu_{14} + \nu_{16} = 1294 \text{ cm}^{-1}$ but not for the 1121-cm^{-1} band as a combination tone. One other possible explanation for ν_6 and ν_7

is that the single strong band at 1151 cm^{-1} is a composite of both bands.

Three of the four assignments for a_u fundamentals deserve comments. For ν_{11} , the spectral evidence for a C-type band centered at 798 cm^{-1} is in the higher pressure segment of the IR spectrum in Figure 4. The P–R width of this band is consistent with a C-type contour, and some suggestive structure, similar to that of the band at 934 cm^{-1} , is seen when the high-pressure scan is spread out. Consistent with the observed low intensity of this band is the prediction of very weak intensity in the calculations. Although residual water lines interfere with the IR spectrum in the vicinity of 227 cm^{-1} , the band in this region is almost certainly of C-type shape and thus appropriate for ν_{12} . The spectral evidence for the band shape at 154 cm^{-1} is less certain. Residual water lines interfere. For the mode of the a_u symmetry species, a choice must be made between this feature and the one at 133 cm^{-1} . The feature at 154 cm^{-1} appears to be a dominant Q branch, as expected for a C-type band. Moreover, the band at 133 cm^{-1} has a width appropriate to a hybrid A/B-type band. In Table 2, bandwidths (P–R spacings) are given in parentheses for many of the IR bands. In addition, the calculated intensity for ν_{13} is weaker than the calculated intensity for ν_{24} , a prediction that is consistent with the relative intensities in the spectrum and the present assignment. The assignment of ν_{24} as 133 cm^{-1} also finds support in explaining the combination tone at 506 cm^{-1} . Overall good agreement exists between the assignments for the a_u modes and the predicted frequencies.

Of the three assignments for b_g modes, doubt attends the assignment of ν_{14} at 897 cm^{-1} in the Raman spectrum. This assignment is based on a band of very weak intensity that appears to be depolarized. The added segment in Figure 5 shows this weak feature at a higher signal level. This choice for ν_{14} is reinforced by the predicted frequency and by the use of ν_{14} in

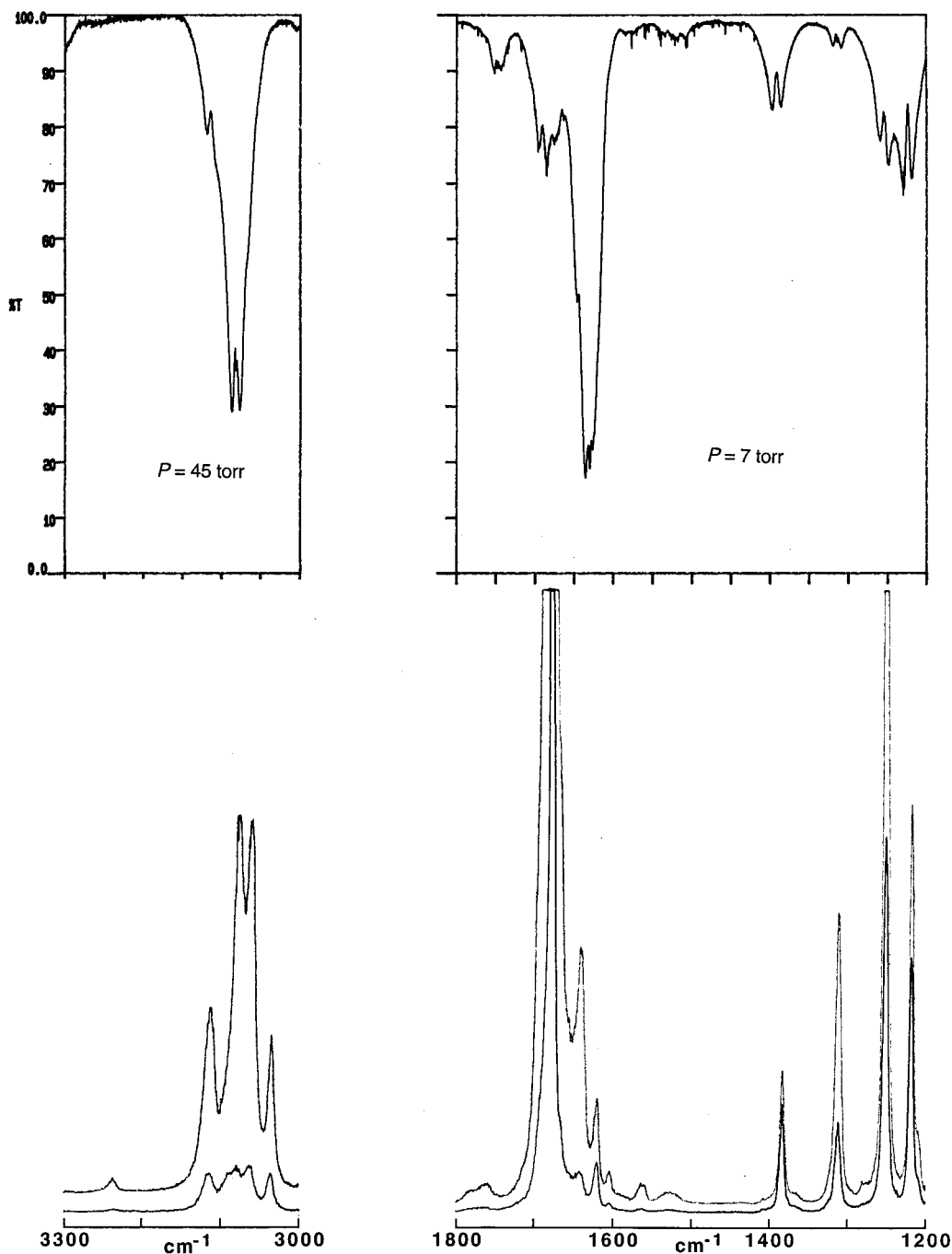


Figure 7. The CH and C=C stretching regions for *cis,trans*-1,4-difluorobutadiene. Gas-phase IR spectrum on top; liquid-phase ($T = -82\text{ }^{\circ}\text{C}$) Raman spectrum on the bottom.

explaining three weak features due to combination tones. Although the depolarization ratio for the band at 830 cm^{-1} in the Raman spectrum appeared to be <0.75 , we conclude that this assignment is correct for ν_{15} .

Among the b_u modes we note that a Fermi resonance probably influences the frequency for ν_{20} . Two features of comparable, weak-medium intensity and B-like shape in the IR spectrum share branches centered at 1299 cm^{-1} , which we adopt as an average value for ν_{20} . Consistent with the observations, a weak intensity was predicted for the transition for this fundamental. An alternative explanation for this broad feature is a C-type band due to the combination tone $\nu_6 + \nu_{13} = 1305\text{ cm}^{-1}$ (A_u). If this combination tone assignment is made, no reasonable feature remains in the IR spectrum to assign to ν_{20} . One other b_u assignment deserves comment. The band at 621 cm^{-1} , which

is assigned to ν_{23} , is broad and tending toward C-type in shape. This distorted shape could be due to a very close Fermi resonance doublet formed with $\nu_{12} + \nu_{16} = 624\text{ cm}^{-1}$. Before the predicted frequencies were available, we had assigned this band to an a_u mode. The predicted frequencies rule out, however, an a_u assignment in this spectral region. Two combination tones, which use ν_{23} at 621 cm^{-1} , reinforce the assignment of ν_{23} .

In summary, all of the assignments of fundamentals of the *trans,trans* isomer seem well supported with experimental data except perhaps for $\nu_{14}(b_g)$, which depends on a very weak feature in the Raman spectrum. In addition, most of the weak features in the spectra are explained as binary combination tones in Table S7 in the Supporting Information. Satisfactory assignments were made for many more weak bands that were observed in higher pressure spectra and in regions not shown in Figures 3 and 4.

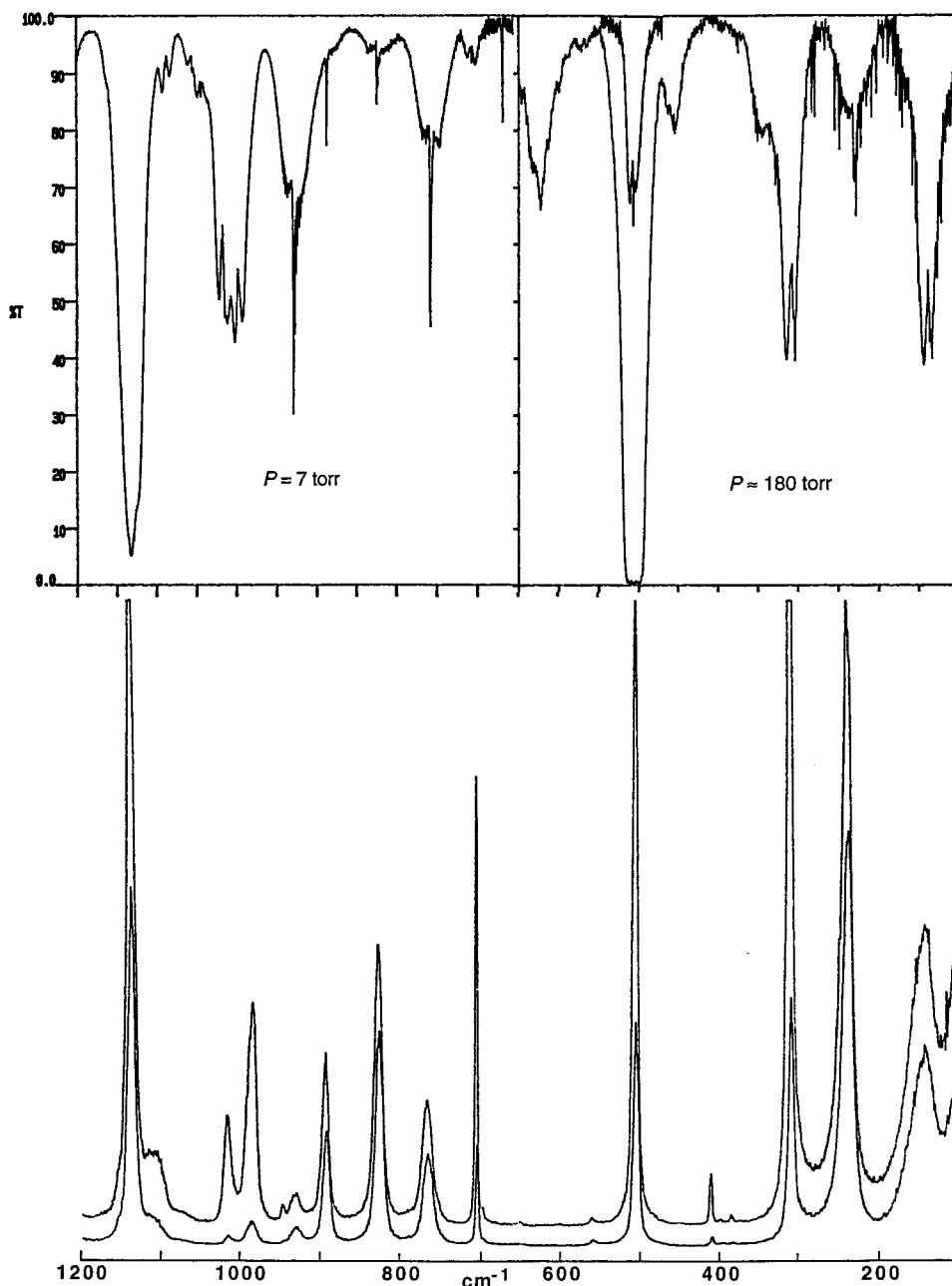


Figure 8. Skeletal motion and low-frequency region for *cis,trans*-1,4-difluorobutadiene.

These additional assignments are in Table S7. Two of the combination bands seen in Figure 4 call for an exceptional explanation. One is the B-type band at 684 cm^{-1} in the IR spectrum, which has been assigned as the difference tone $\nu_{15} - \nu_{13} = 676\text{ cm}^{-1}$ (B_u). The ν_{13} fundamental has a sufficiently low frequency to be populated at room temperature and thus to be involved in an observable difference tone. An alternative assignment as $3 \times \nu_{12} = 681\text{ cm}^{-1}$ (A_u), which, in addition to being a low intensity ternary combination, predicts the wrong band shape. Although difference tones should have exact frequency matches, the use of a liquid-phase value for ν_{15} compromises this accuracy for the gas-phase spectrum. Based on similar reasoning, the difference tone $\nu_{22} - \nu_9 = 705\text{ cm}^{-1}$ is used to explain the 715-cm^{-1} band in the IR spectrum.

Assignment for *cis,cis*-DFBD. Infrared and Raman spectra for *cis,cis*-DFBD are shown on the top and bottom, respectively, in Figures 5 and 6. The added, higher pressure segment for the IR spectrum in Figure 6 supports assigning a weak feature at

914 cm^{-1} as a fundamental. This IR segment was recorded with a sample pressure of 49 Torr. The very weak band at 949 cm^{-1} in this segment with variable relative intensity in the two scans is due to an unidentified impurity. Table 3 provides the assignments of the principal bands observed in the IR and Raman spectra. Sharp lines in the far-IR part of the spectrum are due to residual water. Table 3 also lists all the frequencies and IR intensities as predicted from the ACM calculations. Table S8 in the Supporting Information gives assignments of weak features that are not crucial to identifying fundamentals.

Most of the assignments for the fundamentals of *cis,cis*-DFBD are a direct consequence of applying the selection rules. Consequently, we only comment on the assignments that depend on closer interpretation.

Among the modes of a_g symmetry, the most puzzling assignment is for the second CH stretching mode. One of the CH stretching modes is securely assigned to the strong, polarized Raman band at 3088 cm^{-1} . As seen in Figure 5, there are two

TABLE 4: Observed Vibrational Frequencies and Assignments for *cis,trans*-1,4-Difluorobutadiene (in cm^{-1})

infrared			Raman			predicted ^d		assignment	
gas		<i>I</i> ^c	liquid		<i>I</i> ^c	freq.	<i>I</i> ^c		
freq.	sh. ^b		freq.	pol. ^d				freq.	<i>I</i> ^c
3114	B(10)	m	3114	p	w	3232	w	ν_1 fundamental	a'
3082	A/B(10.2)	m	3078	p	m	3208	m	ν_2 fundamental	a'
~3070	?	w	3062	p	m	3205	w	ν_3 fundamental	a'
			3036	p	w	3190	vw	ν_4 fundamental	a'
1690	B(12)	m	1679	p	vs	1743	m	ν_5 fundamental	a'
1678	B(12)	m						$\nu_{18} + \nu_{21} = 1687$ FR ^e	A'
1629	A/B(9.3)	vs	1621	p	w	1687	vs	ν_6 fundamental	a'
			1605	p	vw			$\nu_8 + \nu_{16} = 1621$ FR ^e	A'
1391	B(12)	m	1385	dp?	w	1421	m	ν_7 fundamental	a'
1313	A/B(10.5)	w	1313	p	m	1339	w	ν_8 fundamental	a'
1253	A/B(12.0)	m	1252	p	s	1282	m	ν_9 fundamental	a'
1224	B(12.4)	m	1219	p	m	1250	m	ν_{10} fundamental	a'
~1155	?	m	1138	p	s	1168	m	ν_{11} fundamental	a'
1129	A/B(10)	vs	1106	p	w	1153	vs	ν_{12} fundamental	a'
1017	B(9)	s	1015	p	w	1023	s	ν_{13} fundamental	a'
998	B(9)	s	984	p	m			$2 \times \nu_{16} = 1008$ FR ^e	A'
929	C(18) ^f	s	930	dp	w	964	s	ν_{18} fundamental	a''
887	C(~18)	m	893	dp	m	921	m	ν_{19} fundamental	a''
824	C(18) ^f	m	826	dp	m	860	w	ν_{20} fundamental	a''
758	C(18)	s	765	dp?	m	779	m	ν_{21} fundamental	a''
706	A(10)	w	704	p	m	719	w	ν_{14} fundamental	a'
						526	w	ν_{22} fundamental	a''
504	A/B(9)	m	505	p	s	510	m	ν_{15} fundamental	a'
~335	B?	vw						$2 \times \nu_{24} \approx 310$ FR ^e	A'
308	B(11)	w	312	p	s	308	vw	ν_{16} fundamental	a'
230	C(~20)	vw	242	dp?	s	236	vw	ν_{23} fundamental	a''
			155	dp?	m	140	vw	ν_{24} fundamental	a''
138	B(10)	w	146	dp?	m	142	w	ν_{17} fundamental	a'

^a See Table 2 except: (a') 3.06, 5.65, 3.16, 0.33, 15.32, 75.24, 8.46, 1.96, 10.69, 15.96, 16.88, 100.00, 59.69, 2.57, 9.56, 0.82, 1.24; and (a'') 25.64, 6.31, 2.57, 16.71, 2.97, 0.46, 0.54. ^{b-c} See Table 2. ^f Hot band structure.

weak, but polarized bands at 3118 and 3047 cm^{-1} that are candidates for the other mode. Neither of these latter two frequencies comes close to a predicted binary combination tone. A combination tone, $\nu_3 + \nu_4 = 3086 \text{ cm}^{-1}$ (A_g), is predicted to be almost coincident with the frequency of the secure CH stretching mode at 3088 cm^{-1} . Fermi resonance of the combination tone with the fundamental could explain either of the weak features. The only basis for making an assignment of the CH stretching mode to 3118 or 3047 cm^{-1} was to compare predicted and observed frequencies for the *trans,trans* and *cis,cis* isomers. The two predicted frequencies for the *cis,cis* isomer (Table 3) average 23 cm^{-1} higher than the corresponding average for the *trans,trans* isomer (Table 2). This comparison led us to assign the higher frequency at 3118 cm^{-1} to the second CH stretching mode of the *cis,cis* isomer. The lower frequency band at 3047 cm^{-1} is then explained as a Fermi resonance outcome. The other questionable assignment for the a_g modes is selecting the weak but polarized Raman band at 1410 cm^{-1} for ν_4 . No other spectral feature is within range of the prediction of 1445 cm^{-1} . Also, the 1410- cm^{-1} band does not have a good, alternative explanation as a combination tone.

For the a_u modes, two assignments can be questioned. One of these is the choice of the weak band at 914 cm^{-1} in the IR spectrum for ν_{10} . This band has a prominent Q branch, which could be interpreted as evidence for an A-type band as well as a C-type band. Furthermore, the combination tone $\nu_8 + \nu_{24} = 916 \text{ cm}^{-1}$ (B_u) could explain an A-type band. The assignment as ν_{10} at 914 cm^{-1} is supported because no other band appears in reasonable agreement with a predicted frequency of 953 cm^{-1} and a very weak predicted intensity. The other a_u assignment that requires comment is the use of the band at 78 cm^{-1} in the IR spectrum for ν_{13} . The shape of this band is obscured by residual water lines and the high signal-to-noise ratio in this

region. Little doubt remains about this band being due to ν_{13} because the next lowest, predicted frequency is quite far away at 162 cm^{-1} .

For the b_g modes, a mild question accompanies assigning ν_{15} to the weak Raman feature at 789 cm^{-1} . This band is, however, clearly observable and depolarized.

The assignments for two modes of b_u symmetry deserve comment. The assignment for ν_{20} depends on a band of medium intensity at 1340 cm^{-1} . This assignment agrees well with the predicted frequency of 1364 cm^{-1} and has the predicted medium intensity. Furthermore, the 1340- cm^{-1} band is not explained well by a combination tone. Though not in doubt as evidence for the ν_{23} fundamental, the exceptional structure in the 630- cm^{-1} region in the IR spectrum deserves discussion. Two features of equal intensity appear in this region. They are split by 24 cm^{-1} , too far to be part of the same band. They are undoubtedly a Fermi resonance doublet, with $\nu_{13} + \nu_{16} = 638 \text{ cm}^{-1}$ being the perturbing state. This explanation rests on assigning ν_{13} (a_u) to the 78 cm^{-1} band and thus reinforces this lowest frequency assignment. The average frequency of the two bands is used for ν_{23} .

In summary, all of the assigned fundamentals for the *cis,cis* isomer seem secure except for the choice between the two weak features in the Raman spectrum for the second CH stretching mode of a_g symmetry and some uncertainty about ν_{10} (a_u), which is based on a weak feature in the IR spectrum. Except for the very weak band at 2998 cm^{-1} , all of the weaker features can be explained as binary combination tones as given in Table S8 in the Supporting Information, thereby providing further support to the assignment of fundamentals. Assignments of many more weak features that were found in spectra at higher pressures and in regions not shown in Figures 5 and 6 are in Table S8.

TABLE 5: Comparison of the Fundamentals of *trans,trans*-1,4-Difluorobutadiene and *trans,trans*-1,4-Dichlorobutadiene (in cm^{-1})

symm. species		approx. descript. ^a	F ₂ BD	Cl ₂ BD ^{b,c}	symm. species		approx. descript. ^a	F ₂ BD	Cl ₂ BD ^{b,c}
a _g	ν_1	sym CH _t str	3091	3068	b _g	ν_{14}	aym CH _c flap	897	[919]
	ν_2	sym CH _c str	3048	3030		ν_{15}	asym CH _t flap	830	860
	ν_3	sym C=C str	1681	1625		ν_{16}	asym CX flap	397	270?
	ν_4	sym CH _c bd	1325	1295	b _u	ν_{17}	asym CH _t str	3086	3075
	ν_5	sym CH _t bd	1280	1285		ν_{18}	asym CH _c str	3056	3030
	ν_6	sym CX str	1151	825		ν_{19}	asym C=C str	1638	1572
	ν_7	CC ctr	1121	1140		ν_{20}	asym CH _c bd	1299	1295
	ν_8	sym C=C-C bd	409	375		ν_{21}	asym CH _t bd	1221	1245
	ν_9	sym CX bd	383	225		ν_{22}	asym CX str	1088	810
a _u	ν_{10}	sym CH _c flap	934	955		ν_{23}	asym CX bd	621	495
	ν_{11}	sym CH _t flap	798	760	ν_{24}	asym C=C-C bd	133	[114]	
	ν_{12}	sym CX flap	227	[176]					
	ν_{13}	torsion	154	[71]					

^a sym = symmetric, asym = antisymmetric with respect to C₂ rotation axis; str = stretching; bd = bending; t = terminal; c = central. ^b Reference 5. ^c Values in brackets were computed in normal coordinate calculations.⁵

Essentially all of these features were explained satisfactorily with binary combinations.

Assignment for *cis,trans*-DFBD. Despite the lower symmetry of the *cis,trans* isomer, the assignments of vibrational fundamentals for this isomer are comparably certain as those for the two more symmetrical isomers. The C_s symmetry makes all fundamentals active in both the IR and Raman spectra, thereby giving two opportunities to observe all of them. The structural variety in the molecule keeps most fundamentals rather well spread out in frequency. There are also some intimations of the relationship to the two more symmetric isomers. Thus, one of the two C=C stretching modes is associated with a high intensity in the Raman spectrum, whereas the other is associated with a high intensity in the IR spectrum. A similar pattern is found for bands related to the two CF stretching modes. As was done for the other two isomers, we discuss only the problematic assignments for the *cis,trans* isomer. The remaining assignments are a direct and convincing consequence of applying the selection rules. The spectra for *cis,trans*-DFBD are shown in Figures 7 and 8. Table 4 gives predictions for frequencies and intensities and gives assignments for the main features in the two spectra of this isomer. Table S9 in the Supporting Information gives assignments for the weaker features and impurities.

Among the bands used for a' modes, five deserve comment. The good, polarized feature of medium intensity in the Raman spectrum at 3036 cm^{-1} is very likely due to ν_4 , even though no counterpart is seen in the IR spectrum. This absence of observable intensity in the IR spectrum is consistent with the very weak intensity predicted in the calculations. The predicted separation of ν_{11} and ν_{12} is the small value of 15 cm^{-1} , consistent with the assignment of a prominent feature for one mode, ν_{11} , at 1138 cm^{-1} in the Raman spectrum and a prominent feature at 1129 cm^{-1} for the other mode, ν_{12} , in the IR spectrum. A weak feature corresponding to ν_{11} may be the remnant of a shoulder seen at 1155 cm^{-1} in the IR spectrum. For ν_{13} , two very close bands of nearly equal intensity are found near 1010 cm^{-1} . The splitting and the intensity pattern is different in the liquid-phase Raman spectrum, but it is expected that the extent of Fermi resonance will be sensitive to small frequency shifts due to the change from the gas phase to the liquid phase. This structure is undoubtedly a consequence of a Fermi resonance interaction with $2\nu_{16} = 1008 \text{ cm}^{-1}$ being the likely perturber. We use an average value of 1008 cm^{-1} for ν_{13} .

For the a'' modes we comment on the assignments for two. No discernible feature is seen for ν_{22} in the IR spectrum. A

very weak, depolarized band at 560 cm^{-1} in the Raman spectrum is a possible candidate for ν_{22} , but this band can be explained as the ternary combination $\nu_{23} + 2\nu_{24} = 552 \text{ cm}^{-1}$. It is unlikely that this band is due to ν_{22} . The frequency of 560 cm^{-1} is much higher than the predicted frequency of 526 cm^{-1} , contrary to all other comparisons of predictions with observations in this lower frequency region. With few exceptions for the set of three isomers, the predicted frequencies are higher than the observed ones. Furthermore, the IR intensity of the band for this fundamental is predicted to be about one-third of that of the band of medium intensity at 504 cm^{-1} , yet no band is found in the vicinity of 560 cm^{-1} in the IR spectrum. Most likely the band for this mode is overlapped by the band due to ν_{15} (a') at 505 cm^{-1} . The A-type band shape in the IR spectrum and the polarized character of the corresponding Raman band indicate, however, that both IR and Raman features must be due principally to the ν_{15} mode.

In the IR spectrum, a C-type band for ν_{24} is not evident at the lowest frequencies. The band for this fundamental is predicted to have very weak intensity and is likely overshadowed by the B-type band for ν_{17} centered at 138 cm^{-1} . The predicted relative IR intensity for ν_{24} is 0.54 in comparison with 1.24 for ν_{17} . The residual water lines in the spectrum may also obscure a weak feature due to ν_{24} . In the Raman spectrum the exceptionally broad and apparently depolarized band near 150 cm^{-1} is probably due to ν_{24} as well as ν_{17} . A band for ν_{17} (a') should be polarized. In a survey scan in the low-frequency region with a Kaiser Optical notch filter in front of the entrance slit, the band in the 150- cm^{-1} region was observed without a sloping baseline. In this trace, a maximum appears at 155 cm^{-1} , rather too high for the Raman counterpart of the IR band at 138 cm^{-1} . Furthermore, assigning the combination tone that appears at $\sim 335 \text{ cm}^{-1}$, on the high-frequency side of the band at 308 cm^{-1} , calls for a frequency of $\sim 155 \text{ cm}^{-1}$. If ν_{24} is about 155 cm^{-1} , then $2\nu_{22} = 310 \text{ cm}^{-1}$. Fermi resonance could then produce the somewhat higher frequency feature that is seen in the spectrum. No other reasonable explanation exists for the feature at $\sim 335 \text{ cm}^{-1}$. In addition, several other combination tones have better agreement between observed frequencies and predictions with use of the higher frequency for ν_{24} . The close proximity of the broad band in the Raman spectrum to the predicted frequencies of 142 and 140 cm^{-1} for the two modes makes the overlap interpretation all the more likely to be correct.

In summary, the assignments for all 17 a' fundamentals for *cis,trans*-DFBD seem quite secure. For five of the seven a'' modes, the assignments are certain. No direct spectral evidence

TABLE 6: Comparison of the Fundamentals of *cis,cis*-1,4-Difluorobutadiene and *cis,cis*-1,4-Dichlorobutadiene (in cm^{-1})

symm. species		approx. descript. ^a	F ₂ BD	Cl ₂ BD ^{b,c}	symm. species		approx. descript. ^a	F ₂ BD	Cl ₂ BD ^{b,c}	
a _g	ν_1	sym CH _t str	3118	3085	b _g	ν_{14}	aym CH _c flap	897	913	
	ν_2	sym CH _c str	3088	3040		ν_{15}	asym CH _t flap	789	[746]	
	ν_3	sym C=C str	1676	1625		ν_{16}	asym CX flap	580	500	
	ν_4	sym CH _c bd	1410	1415		b _u	ν_{17}	asym CH _t str	3109	3095
	ν_5	sym CH _t bd	1248	1232			ν_{18}	asym CH _c str	3092	3058
	ν_6	sym CX str	1134	733			ν_{19}	asym C=C str	1624	1574
	ν_7	CC ctr	946	1063			ν_{20}	asym CH _c bd	1340	1305
	ν_8	sym C=C—C bd	751	670			ν_{21}	asym CH _t bd	1215	1185
	ν_9	sym CX bd	232	186			ν_{22}	asym CX str	1044	777
a _u	ν_{10}	sym CH _c flap	914	932	ν_{23}	asym CX bd	632	495		
	ν_{11}	sym CH _t flap	762	703	ν_{24}	asym C=C—C bd	165	[114]		
	ν_{12}	sym CX flap	330	[320]						
	ν_{13}	torsion	78	[47]						

^{a-c} See Table 5.**TABLE 7: Comparison of the Fundamentals of *cis,trans*-1,4-Difluorobutadiene and *cis,trans*-1,4-Dichlorobutadiene (in cm^{-1})**

symm. species		approx. descript. ^a	F ₂ BD	Cl ₂ BD ^{b,c}	symm. species		approx. descript. ^a	F ₂ BD	Cl ₂ BD ^{b,c}
a'	ν_1	CH _t str	3114	3095	a''	ν_{13}	CC str	1008	1090
	ν_2	CH _t str	3082	3073		ν_{14}	sym C=C—C bd	706	599
	ν_3	sym CH _c str	3062	3037		ν_{15}	CX bd	504	395
	ν_4	asym CH _c str	3036	3037		ν_{16}	CX bd	308	[257]
	ν_5	sym C=C str	1690	1617		ν_{17}	asym C=C—C bd	138	[87]
	ν_6	asym C=C str	1629	1572		ν_{18}	asym CH _c flap	929	950
	ν_7	CH _t bd	1391	1365		ν_{19}	sym CH _c flap	887	908
	ν_8	CH _t bd	1313	1340		ν_{20}	CH _t flap	824	810
	ν_9	sym CH _c bd	1253	1287		ν_{21}	CH _t flap	758	712
	ν_{10}	asym CH _c bd	1224	1235		ν_{22}	=CHX (cis)	[526] ^d	452
	ν_{11}	CX str	1138	855		ν_{23}	=CHX (trans)	230	190
	ν_{12}	CX str	1129	765		ν_{24}	torsion	155	[104]

^a sym = symmetric; asym = antisymmetric with respect to center of C—C bond; str = stretching; bd = bending; t = terminal; c = central. ^{b,c} See Table 5. ^d Prediction from results of ACM calculations.

exists for ν_{22} , and the evidence for ν_{24} , though tangible, is questionable. With the exception of the use of two ternary combination tones, all of the weak features seen in the spectra in Figures 7 and 8 are explained as binary combination tones. The assignments for these weak features are given in Table S9 in the Supporting Information. As was true for the other two isomers, assignments for many other weak features observed at higher pressures or in regions not depicted in Figures 7 and 8 are in Table S9.

Discussion

The pattern of intensities of C-type bands in the gas-phase IR spectra that were used by Viehe and Franchimont¹ in their initial identification of the three isomers of DFBD is amply confirmed in our higher resolution spectra. In Figure 4 for *trans,trans*-DFBD, which has only the trans HC=CH configuration, the band at 934 cm^{-1} is strong, whereas the band at 798 cm^{-1} is weak. In contrast, in Figure 6 for *cis,cis*-DFBD, which has only the cis HC=CH configuration, the band at 914 cm^{-1} is weak, whereas the band at 762 cm^{-1} is strong. Of course, for each of these isomers, the other two out-of-plane CH flapping modes are Raman active only. The pattern of intensities just described is the same as that observed in the IR spectra of *cis*- and *trans*-1,2-difluoroethylene.¹⁵ For the *cis*-*trans* isomer of DFBD, which has both *cis* and *trans* HC=CH configurations, the bands at 929 and 758 cm^{-1} are both strong. The IR bands of C-type shape and medium intensity are also at 887 and 824 cm^{-1} . These weaker bands correspond to the Raman-active modes of the two more symmetric isomers.

The stronger C-type bands of the nonpolar isomers are also of particular interest because the rotational structure of these

bands appears to be analyzable and thus the source of information about the structure of the two isomers. In Figures 4 and 6, evidence of many Q branches of subbands can be seen for the bands at 934 and 762 cm^{-1} in these spectra of moderate resolution. For the *trans,trans* isomer, we have already made considerable progress in analyzing the C-type band at 934 cm^{-1} in the high-resolution IR spectrum. The spectrum was recorded at 0.002 cm^{-1} resolution by Dr. Michael Lock at Justus Liebig University in Giessen, Germany. Preliminary values of the ground-state rotational constants are 1.0508, 0.038972, and 0.037580 cm^{-1} from the analysis of the rotational structure in the high-resolution spectrum. These values give 16.04, 432.56, and 448.58 $\text{amu} \text{ \AA}^2$ for the principal moments of inertia, which are in reasonable agreement with those in Table 1 that were predicted by the calculations.

Although the frequencies predicted from the calculations have been used in developing the assignment of the three isomers of DFBD, the majority of the assignments were secured by application of the selection rules and standard frequency correlations. With the exception of the CH stretching frequencies, which are strongly influenced by anharmonicity, the agreement between the observations and the calculations is very good. Thus, the overall good agreement of the observed fundamental frequencies and the predicted values is strong evidence that the hybrid Hartree–Fock/density–functional theory ACM method of making frequency predictions, *without scaling*, is remarkably good.

Tables 5, 6, and 7 provide summaries of the vibrational fundamentals of the three isomers of DFBD. These tables include the corresponding assignments for the three isomers of 1,4-dichlorobutadiene.⁵ With allowance for the marked differ-

ences in frequencies for modes that are significantly CF or CCl in character, the correlation between the two assignments is strikingly good. It must be emphasized that the existing assignments for the dichlorobutadienes were not consulted in making the assignments for the DFBD isomers. The qualitative characterizations of the normal modes in terms of symmetry coordinates that are given in Tables 5, 6, and 7 are based on the normal coordinate calculations of Benedetti et al.⁵ for the three 1,4-dichlorobutadienes and on the strong correlation between the frequencies of the two sets of isomers. The strong correlation between the assignments for the isomers of DFBD and 1,4-dichlorobutadiene reinforces the conclusion that the fundamentals for the three isomers of DFBD have been correctly assigned.

One significant frequency difference appears between the fundamentals of the three isomers of DFBD. The frequency for the torsion of the C–C bond of the cis,cis isomer is only 78 cm⁻¹, whereas it is 155 and 154 cm⁻¹ for the other two isomers. If this difference is a consequence of less dispersed double bond character in the cis,cis isomer, one would expect this effect to be reflected also in the frequencies for C=C stretching. Yet, the average values for the two C=C modes of the three isomers are <10 cm⁻¹ apart. Thus, it seems likely that the greater ease of torsion for the cis,cis isomer is the expected consequence of steric crowding in this isomer, a result that seems at odds with this isomer having the lowest energy of the three isomers.

We look forward to obtaining complete structures for the three isomers of DFBD and to finding correlations between structural adjustments and the curious energetics. A deeper normal coordinate analysis could also be fruitful. For the structural studies, we have been preparing various deuterated species by exchange with basic deuterium oxide. These deuterated species would also be useful in supporting a normal coordinate analysis.

Summary

Essentially complete assignments have been obtained for the 24 vibrational fundamentals of each of the three isomers of DFBD in s-trans conformations. Experimental observations were supplemented with frequencies predicted from the results of geometry optimization by hybrid Hartree–Fock/density–functional theory ACM calculations. Overall, these unscaled predictions of vibrational frequencies were quite good. With a few exceptions, all of the observed frequencies in the spectra

were attributable to the s-trans rotamers. Thus, no evidence for the higher energy s-gauche rotamers was found. Strong C-type bands in the spectra of the nonpolar trans,trans and cis,cis isomers, which are near-prolate symmetric tops, are good candidates for rotational analysis of bands in high-resolution IR spectra to yield detailed structural information.

Acknowledgment. We are indebted to Sonan Osmani for first observing the stereospecific thermal isomerization of *trans*-3,4-difluorocyclobutene when he was investigating exchange reactions in basic D₂O. We are also indebted to David C. Oertel for investigating the NMR spectra of the three isomers. The research was supported by grant 30937-B4 from the Petroleum Research Fund of the American Chemical Society.

Supporting Information Available: Tables S1–S6 contain the Cartesian coordinates and the resulting geometric parameters of the three isomers of DFBD obtained from the ACM calculations. Tables S7–S9 contain the assignments of combination tones and of other weak features due to impurities for the trans,trans, cis,cis, and cis,trans isomers, respectively. This material is available free of charge via the Internet at <http://pubs.acs.org>.

References and Notes

- (1) Viehe, H.-G. *Angew. Chem., Internat. Ed.* **1963**, *2*, 622.
- (2) Viehe, H.-G.; Franchimont, E. *Chem. Ber.* **1964**, *97*, 602.
- (3) These isomerizations were done in benzene solution in sealed tubes. Qualitatively, the results of our gas-phase isomerizations give similar ratios.
- (4) Becke, A. D. *J. Chem. Phys.* **1993**, *98*, 6548.
- (5) Benedetti, E.; Aglietto, M.; Vergamini, P.; Aroca Muñoz, R.; Rodin, A. V.; Panchenko, Yu. N.; Pentin, Yu. A. *Spectrochim. Acta* **1976**, *34*, 21.
- (6) Wiberg, K. B. *Acc. Chem. Res.* **1996**, *29*, 229.
- (7) Engkvist, O.; Karlström, G.; Widmark, P.-O. *Chem. Phys. Lett.* **1997**, *25*, 19.
- (8) Craig, N. C.; Appleman, R. A.; Barnes, H. E.; Morales, E.; Smith, J. A.; Klee, S.; Lock, M.; Mellau, G. C. *J. Phys. Chem. A* **1998**, *102*, 6745.
- (9) Craig, N. C.; Hawley, S. E.; Lee, L. V.; Pearson, A. *Spectrochim. Acta* **1994**, *50A*, 191.
- (10) Kirmse, W.; Rondan, N. G.; Houk, K. N. *J. Am. Chem. Soc.* **1984**, *106*, 7989.
- (11) Ahlrichs, R.; Bär, M.; Ehrig, M.; Häser, M.; Horn, H.; Kölmel, C. TURBOMOLE 400, Molecular Simulations, Inc., San Diego, CA, 1996.
- (12) Schäfer, A.; Horn, H.; Ahlrichs, R. *J. Chem. Phys.* **1992**, *93*, 2571.
- (13) Huber-Wälchli, P.; Günthard, H. *Spectrochim. Acta* **1981**, *A37*, 285.
- (14) De Maré, G. R.; Panchenko, Yu. N.; Vander Auwera, J. *J. Phys. Chem.* **1997**, *101*, 3998.
- (15) Craig, N. C.; Overend, J. *J. Chem. Phys.* **1969**, *51*, 1127.